The $P450_{cam}$ G248E Mutant Covalently Binds Its Prosthetic Heme Group†

Julian Limburg,‡ Laurie A. LeBrun,§ and Paul R. Ortiz de Montellano*

Department of Pharmaceutical Chemistry, University of California, San Francisco, California 94143-0446

Received October 29, 2004; Revised Manuscript Received January 12, 2005

ABSTRACT: Previous studies on mammalian peroxidases and cytochrome P450 family 4 enzymes have shown that a carboxylic group positioned close to a methyl group of the prosthetic heme is required for the formation of a covalent link between a protein carboxylic acid side chain and the heme. To determine whether there are additional requirements for covalent bond formation in the P450 enzymes, a glutamic acid or an aspartic acid has been introduced into $P450_{cam}$ close to the heme 5-methyl group. Spectroscopic and kinetic studies of the resulting G248E and G248D mutants suggest that the carboxylate group coordinates with the heme iron atom, as reported for a comparable $P450_{BM3}$ mutant [Girvan, H. M., Marshall, K. R., Lawson, R. J., Leys, D., Joyce, M. G., Clarkson, J., Smith, W. E., Cheesman, M. R., and Munro, A. W. (2004) *J. Biol. Chem*. *279*, 23274−23286]. The two $P450_{cam}$ mutants have low catalytic activity, but in contrast to the $P450_{BM3}$ mutant, incubation of the G248E (but not G248D) mutant with camphor, putidaredoxin, putidaredoxin reductase, and NADH results in partial covalent binding of the heme to the protein. No covalent attachment is observed in the absence of camphor or any of the other reaction components. Pronase digestion of the G248E $P450_{cam}$ mutant after covalent attachment of the heme releases 5-hydroxyheme, establishing that the heme is covalently attached through its 5-methyl group as predicted by in silico modeling. The results establish that a properly positioned carboxyl group is the sole requirement for autocatalytic formation of a heme−protein link in P450 enzymes, but also show that efficient covalent binding requires placement of the carboxyl close to the methyl but in a manner that prevents strong coordination to the iron atom.

The cytochromes P450, a ubiquitous superfamily of heme-containing monooxygenases, are involved in a wide range of physiological transformations (*1*−*3*). Many of these transformations involve the hydroxylation of hydrocarbons, but the enzymes are generally promiscuous and readily oxidize a broad spectrum of substrates and functionalities. The crystal structures of approximately a dozen P450 enzymes are now available, but the prototypical and best characterized in terms of both mechanism and structure is $P450_{cam}$,[1] an enzyme from *Pseudomonas putida* that normally oxidizes camphor to 5-*exo*-hydroxycamphor (*4*−*6*). In $P450_{cam}$, as in all P450 enzymes for which structures are available, the proximal ligand to the heme iron atom is a highly conserved cysteine thiolate and the distal ligand in the resting ferric state is a water molecule (*4*). With a few exceptions, all P450 enzymes require a set of NADH- or NADPH-dependent redox proteins to provide reducing equivalents to the heme center (*7*). In the case of $P450_{cam}$, the reducing equivalents are provided by putidaredoxin (Pd), an iron−sulfur protein, and putidaredoxin reductase (PdR), an NADH-dependent flavoprotein (*8*, *9*).

Scheme 1: Catalytic Cycle of Cytochrome P450[a]

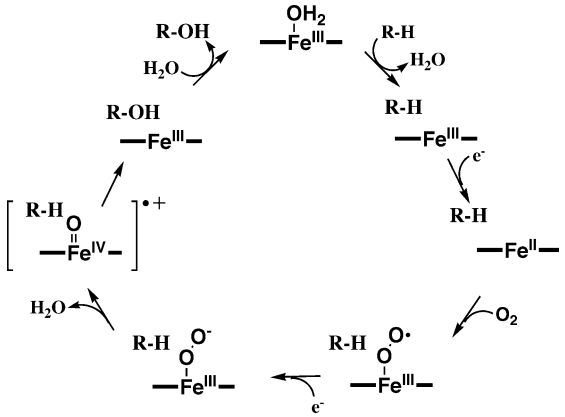

[a] The iron structure represents the heme group of cytochrome P450, RH a hydrocarbon substrate, and R-OH the resulting hydroxylated product.

In the current consensus mechanism for substrate hydroxylation by P450 enzymes (Scheme 1), substrate binding is associated with changes in conformation and active site hydration that result in the loss of the distal water ligand and a shift from the six-coordinate, low-spin Fe(III) heme to the pentacoordinate, high-spin state (*10*, *11*). In $P450_{cam}$, as in most P450 enzymes, this spin flip alters the redox potential of the heme and facilitates reduction of the Fe(III) to Fe(II) by the redox partner (*12*). Following reduction to

† This work was supported by National Institutes of Health Grant GM25515.

* To whom correspondence should be addressed: University of California, San Francisco, 600 16th St., N572D, San Francisco, CA 94143-2280. Telephone: (415) 476-2903. Fax: (415) 502-4728. E-mail: ortiz@cgl.ucsf.edu.

‡ Current address: Department of Chemistry, The University of Kansas, Lawrence, KS 66045.

§ Current address: Anadys Pharmaceuticals, San Diego, CA 92121.

[1] Abbreviations: heme, iron protoporphyrin IX regardless of oxidation and ligation state; $P450_{cam}$, CYP101; TFA, trifluoroacetic acid; Pd, putidaredoxin; PdR, putidaredoxin reductase; 5-HO heme, 5-hydroxymethylheme.

10.1021/bi047686i CCC: $30.25
Published on Web 02/08/2005

Scheme 2: Proposed Mechanism for Covalent Binding of the Heme to the Protein during Catalytic Turnover of the CYP4 P450 Enzymes Involving Oxidation of the Glutamic Acid Carboxylate Group to a Radical, Followed by Hydrogen Abstraction from the Heme Methyl, Internal Electron Transfer To Generate the Cation, and Trapping of the Cation by the Regenerated Carboxylate Anion

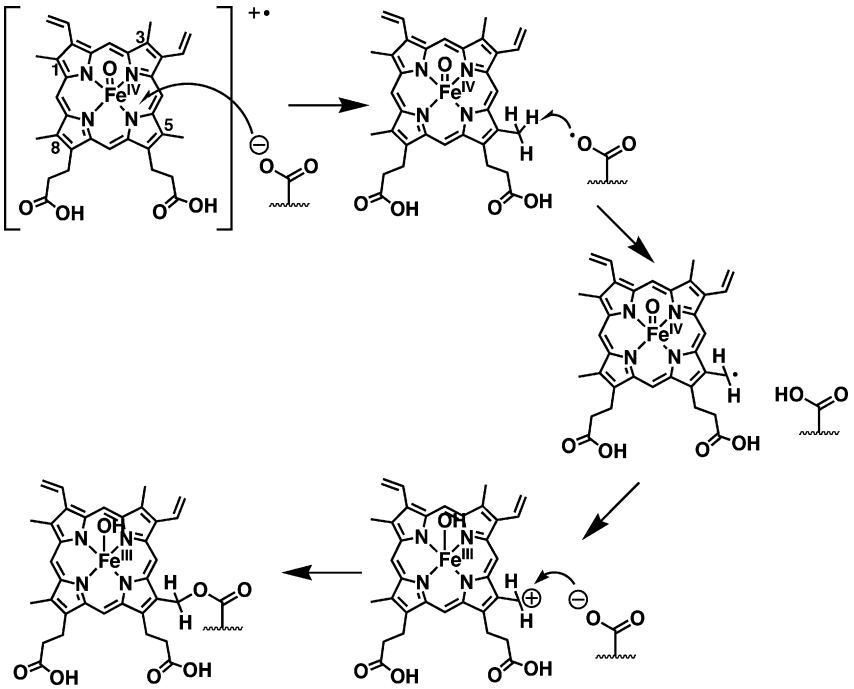

Fe(II), the heme can react with O_2 to form what is formally an Fe(III)−superoxide complex (*5*). A second reducing equivalent reduces this P450 complex to the Fe(III)−hydroperoxide state (*5*). The next step in the catalytic process is normally heterolysis of the O−O bond to give what is thought to be a highly reactive Fe(IV)═O porphyrin radical cation (*6*, *13*). This ferryl intermediate then reacts with the substrate, in the case of a hydrocarbon by abstracting a hydrogen atom, leading to a rebound reaction in which the resulting hydrocarbon radical and an Fe(IV)−OH species recombine to give the hydroxylation product (*13*). Product release then returns the enzyme to its resting state.

In $P450_{cam}$, as in the vast majority of P450 enzymes, the heme cofactor is dissociable, as the only direct interactions between the heme and the peptide chain are the bond between the Fe and the cysteine thiolate ligand and ionic, hydrophobic, and van der Waals interactions of the porphyrin framework with active site residues (*5*). The only known exceptions are the members of the extensive CYP4 family of mammalian fatty acid hydroxylases (*14*−*18*). Thus, in rat liver CYP4A3, an ester linkage is formed between a methyl group of the heme and a glutamate residue, Glu318 (*14*). Subsequent studies of CYP4A3 and CYP4A8, in which the glutamate is conserved, established that the site of esterification on the heme is the C5 methyl group (*17*). Mutation of the glutamate to an alanine precludes formation of the covalent link. Although some of the resulting CYP4 mutants without the covalent heme bond are virtually inactive, others (e.g., CYP4A1 and CYP4A11) retain most of their catalytic activity (*17*). This covalent attachment mirrors that observed in the mammalian peroxidases, in which the heme is covalently linked to the protein through ester bonds to two of the heme methyl groups (*19*−*21*). In contrast to the P450 enzymes, in which the function of covalent heme attachment remains uncertain, in the peroxidases covalent linking of the heme to the protein is absolutely required for catalytic activity (*20*).

Formation of the heme−protein ester bond in both the P450 enzymes and mammalian peroxidases has been proposed to result from an autocatalytic process initiated by formation of the Fe(IV)═O porphyrin radical cation ("Compound I") (*16*−*18*, *20*). The first step of the probable mechanism for covalent heme binding is oxidation of the glutamate to a carboxylic radical with concomitant reduction of the porphyrin radical cation to give the Fe(IV)═O species ("Compound II"). Abstraction of a hydrogen atom from the heme 5-methyl by the carboxyl radical then yields a methylene radical that, through an internal electron transfer, is converted to a carbocation (Scheme 2). Trapping of the carbocation by the glutamate carboxylate directly yields the ester. An alternative, but less likely, mechanism involves deprotonation of the 5-methyl of Compound I by the carboxylate anion followed by two intramolecular electron transfers to give the same carbocation intermediate. Both of these mechanisms require the formation of Compound I or its P450 equivalent.

A corollary of the proposed autocatalytic mechanism is that any P450 enzyme with a suitably positioned glutamic acid residue should be able to form an ester bond to a heme methyl group. This assumes, however, that no other feature of the active site is specifically required for heme−protein cross-linking. This laboratory has recently demonstrated with a mutant of horseradish peroxidase in which a properly located phenylalanine was replaced with a glutamic acid that this is indeed the case for the mammalian peroxidases (*21*). In the P450 arena, a test of the hypothesis was attempted with $P450_{BM3}$ by introducing a glutamic acid residue into the active site at the position (A246E) equivalent to that

Table 1: Sequence Alignment of the I Helices of $P450_{cam}$ and the CYP4A Enzymes from Humans (CYP4A11) and Rats (CYP4A1, -4A2, -4A3, and -4A8)

Protein	Alignment of the I-Helices
	248
$P450_{cam}$	SDEAKRMCGLLLV***G***GLDTVVNFLSFSMEFLAK
	321[a]
CYP4A11	DKDLRAEVDTFMF***E***GHDTTASGISWILYALAT
CYP4A1	DKDLRAEVDTFMF***E***GHDTTASGVSWIFYALAT
CYP4A2	DEDLRAEVDTFMF***E***GHDTTASGSGISWVFYAL
CYP4A3	DEDLRAEVDTFMF***E***GHDTTASGISWVFYALAT
CYP4A8	DKDLRAEVDTFMF***E***GHDTTASGISWIFYALAT

[a] Numbered residue E321 is for CYP4A11. The numbers for the other glutamic acid residues vary slightly.

occupied by the glutamic acid in the CYP4 enzymes (*22*, *23*). It was found that the carboxylate was coordinated to the iron, and although a low catalytic activity was observed, no heme−protein covalent bonding occurred. In the study presented here, we have mutated Gly248 in CYP101 to both Glu and Asp and report here that, as in $P450_{BM3}$ (*22*, *23*), the carboxylate appears to bind to the heme iron. However, both the G248E and G248D mutants retain low camphor hydroxylating activity, and in the case of the G248E mutant, the heme becomes covalently bound to the polypeptide via an ester linkage to the C5 methyl group. These results provide clear evidence that (a) covalent attachment of the heme to the peptide chain in CYP4A enzymes proceeds via an autocatalytic mechanism, (b) the only critical requirement for successful attachment is juxtaposition of the carboxylate group and the heme methyl, and (c) efficient covalent binding, as in the CYP4 enzymes, requires positioning of the carboxyl side chain to allow covalent binding without allowing its coordination to the heme iron.

EXPERIMENTAL PROCEDURES

Materials. 5-OH heme was obtained from a Pronase digest of CYP4A3 as previously described (*17*). All other chemicals were obtained from Sigma (St. Louis, MO). All enzyme manipulations were carried out at pH 7.4 (20 mM potassium phosphate and 100 mM KCl) unless otherwise stated. The wild-type $P450_{cam}$, Pd, and PdR were expressed and purified as previously reported (*26*). Wild-type and mutant $P450_{cam}$ were desalted prior to each reaction using a PD-10 column (Amersham Biosciences, Piscataway, NJ).

Structure Modeling. The 1.8 Å resolution structure of $P450_{cam}$ was used to model a glutamic acid into helix I at position 248 (*5*), the position that corresponds to Glu321 in CYP4A11 when the sequences are aligned (Table 1) (*24*). The point mutation was modeled into the $P450_{cam}$ structure using SYBYL (Tripos Associates).

Preparation of the $P450_{cam}$ G238E/C334A and G248D/C334A Double Mutants. The C334A $P450_{cam}$ gene, prepared as previously described (*25*), was kindly provided by L. Wong (Oxford University, Oxford, U.K.). The $P450_{cam}$ gene was excised from the pCWori/$P450_{cam}$ plasmid by digesting it with *Nde*I and *Xba*I restriction enzymes. The $P450_{cam}$ gene was then subcloned into the pUC19 vector, and this plasmid was used for mutagenesis. The following primers were used to prepare the mutants. Underlined codons represent the base pair changes that were made to affect the amino acid point mutations. For the $P450_{cam}$ G248E mutant, the forward primer was 5′GC CTG TTA CTG GTC GAG GGC CTG GAT ACG G3′ and the reverse primer was 5′CG GAC AAT GAC CAG CTC CCG GAC CTA TGC C3′. For the $P450_{cam}$ G238D mutant, the forward primer was 5′GC CTG TTA CTG GTC GAC GGC CTG GAT ACG G3′ and the reverse primer was 5′C CGT ATC CAG GCC CTC GAC CAG TAA CAG GC3′. The mutations were confirmed by sequence analysis. The mutated $P450_{cam}$ genes were excised, reinserted into the pCWori plasmid, and then used for protein expression and purification as previously reported (*26*).

Spectroscopic Methods. Reduced CO difference and absolute spectra were recorded on a Hewlett-Packard 8452 diode array spectrophotometer. For formation of reduced CO species, a solution of $P450_{cam}$ (wild-type, G248E, or G248D) was placed in a cuvette with a sidearm equipped with a stopcock for introduction of gases, and a second chamber that contained a few milligrams of sodium dithionite (excess). The cuvette was sealed with a rubber septum, and the enzyme solution was purged under a stream of N_2 for 15 min. After purging was complete, the enzyme solution was mixed with the dithionite and then CO was introduced into the cuvette. The P450 content was determined using the method of Omura and Sato (*27*). In the absence of independently determined absorbance coefficients for the proteins with covalently bound heme, we have assumed that the coefficients are the same as for the wild type ($\epsilon \sim 100\,000\ M^{-1}\ cm^{-1}$ for the Soret band). Substrate binding data were collected on a Varian Cary 1E UV−visible dual-beam spectrophotometer. To obtain substrate binding difference spectra, camphor dissolved in ethanol was titrated into the protein sample. The ethanol concentration in the final sample was ≤3%. The spectral binding constant K_s was determined from the hyperbolic plot of the peak to trough absorbance change versus the ligand concentration.

HPLC−UV Analysis of the $P450_{cam}$ G248E Protein. Prior to injection, protein samples were desalted into distilled H_2O, TFA was added to a final concentration of 0.1% (v/v), and the concentration of the solution was made 30% (v/v) in acetonitrile (containing 0.05% TFA). The samples were analyzed on an HP 1090 Series II LC instrument equipped with a diode array detector and a VYDAC protein C4 column (5 mm × 150 mm). The solvent gradient consisted of a mixture of buffer A (0.1% TFA in water) and buffer B (0.05% TFA in acetonitrile) with a flow rate of 1 mL/min. The bound and unbound heme species were separated with a linear stepwise gradient of 30% buffer B for 5 min, from 30 to 50% buffer B from 5 to 25 min, from 50 to 95% buffer B from 25 to 35 min, 95% buffer B from 35 to 50 min, and then adjusted back to 30% buffer B for 10 min. The free heme eluted at 16 min and the bound heme around 28 min. The heme group and protein were monitored at 400 and 280 nm, respectively. The amount of bound heme was calculated from the areas of the 400 nm peaks at 16 and 28 min.

Autocatalytic Reaction. The $P450_{cam}$ G248E mutant (approximately 15 μM) was incubated with 2 mM NADH, 30 μM Pd, 15 μM PdR, and 1 μM catalase for 3 h at 37 °C in the presence and absence of camphor (1.1 mM). The

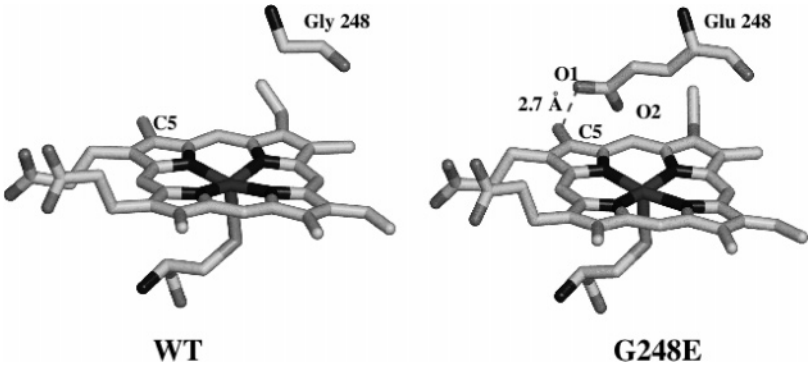

FIGURE 1: Active site of camphor-bound wild-type $P450_{cam}$ showing the position of Gly248 (PDB entry 1DZ4), at left. Model of the active site of G248E $P450_{cam}$ showing that O_1 of Glu248 could be as close as 2.7 Å to the C_5 methyl group of the heme, at right. This figure was generated using PYMOL (*33*).

percentage of covalently bound heme was analyzed by the HPLC procedure described above. The time dependence of covalent heme binding was monitored for the reaction of 2 mM NADH, 30 μM Pd, 15 μM PdR, 1.1 mM camphor, and 1 μM catalase incubated at 37 °C. The samples removed at various times for HPLC analysis were first quenched by desalting into distilled water.

Gas Chromatographic Analysis of Product Formation. Wild-type (1 μM), G248E (100 μM), or G248D (15 μM) $P450_{cam}$ was mixed with 2 mM NADH, 30 μM Pd, 15 μM PdR, 1 μM catalase, and 1.1 mM camphor (final volume of 2 mL) and incubated at 37 °C. For the G248E and G248D mutants, the substrate and product were extracted with CH_2Cl_2 (3 × 200 μL) from 200 μL aliquots of the incubation mixture taken at increasing time points up to 3 h. For the wild type, a single aliquot was taken after 30 min. The $CHCl_2$ layer was dried over anhydrous $MgSO_4$, concentrated to <50 μL, and injected onto an HP 5980 series II gas chromatograph equipped with an Agilent Technologies (Palo Alto, CA) DB-10 capillary column. A 20 min linear temperature gradient from 40 to 280 °C was employed. On the basis of the control reaction using wild-type $P450_{cam}$ (*28*), camphor eluted at 6.8 min and 5-*exo*-hydroxycamphor at 9.8 min.

Pronase Digestion of G248E $P450_{cam}$ and CYP4A3. The solution of G248E (15 μM) after autocatalysis (see above) was concentrated 5-fold (final volume of 200 μL) and loaded onto a Sephadex G25 column (7.5 mL). The proteins were eluted with digestion buffer (50 mM Tris, pH 8.0), and samples with an $r/z > 0.8$ were collected. Pure wild-type $P450_{cam}$, G248E $P450_{cam}$, and CYP4A3 (all as isolated) were exchanged into digestion buffer (50 mM Tris, pH 8.0) and diluted to a concentration of 10 μM. Pronase (1 mg/mL, containing calcium acetate), from a 20 mg/mL stock solution, and imidazole (15 mM) were added to each sample followed by incubation for 18 h at 37 °C.

HPLC Analysis of the Digested Products. Following digestion, the P450 samples were made up to 15% acetonitrile (v/v) containing 0.1% TFA (v/v). The samples (200 μL) were loaded directly onto a VYDAC C4 column (0.5 mm × 150 mm). The solvent gradient consisted of a mixture of buffer A (0.1% TFA in water) and buffer B (0.1% TFA in acetonitrile) with a flow rate of 1 mL/min. Heme and 5-HO heme were separated with a linear stepwise gradient of 15% buffer B for 5 min, from 15 to 40% buffer B from 5 to 25 min, from 40 to 95% buffer B from 25 to 35 min, and 95% buffer B from 35 to 50 min, followed by adjustment back to 15% buffer B for 10 min. 5-HO heme eluted at 27 min, and heme eluted at 32 min.

Table 2: Distance between the Carboxyl Oxygens and the Heme Methyls and Fe in the $P450_{cam}$ G248E and G248D Models

$P450_{cam}$ mutant	carboxyl oxygen	distance to methyl groups and Fe of the heme (Å)				
		1-CH_3	3-CH_3	5-CH_3	8-CH_3	Fe
G248E	O_1	9.9	5.9	2.7	9.5	4.5
	O_2	10.3	7.8	3.1	8.7	5.0
G248D	O_1	10.3	7.1	4.4	8.6	4.0
	O_2	8.1	8.3	5.4	7.7	5.6

LC−MS Analysis of the Digested Products. Following digestion, the concentrations of the P450 samples were made 40% in methanol and formic acid was added to a final concentration of 0.1% (v/v). LC−MS was performed on a Waters Micromass ZQ apparatus coupled to a Waters Alliance HPLC system (2695 separations module, Waters 2487 dual absorbance detector) equipped with an Xterra MS C18 column (2.1 mm × 50 mm). The samples (75 μL) were injected directly onto the C18 column. The solvent gradient consisted of a mixture of 0.1% formic acid in water (buffer A) and 0.1% formic acid in methanol (buffer B) with a flow rate of 0.2 mL/min. The heme species were separated with a linear stepwise gradient of 45% buffer B for 2 min (from 0 to 2 min), from 45 to 70% buffer B from 2 to 12 min, 95% buffer B from 12.1 to 15 min, and 45% buffer B from 15.1 to 17 min. The detector was set at 400 nm. The MS settings were as follows: capillary voltage, 3.5 kV; cone voltage, 50 V; desolvation temperature, 250 °C; source temperature, 120 °C; and ionization mode, ES+. 5-OH-heme eluted at 12 min and heme at 14 min.

RESULTS

Model. In CYP4A11, the heme is covalently linked to the protein via an ester linkage to Glu321 in helix I (*14*, *17*). An alignment of the sequences of the I helices of $P450_{cam}$, human CYP4A11, and rat isoforms CYP4A1, -4A2, -4A3, and -4A8 shows that the equivalent position in $P450_{cam}$ is Gly248 (Table 1). In the computer model of the $P450_{cam}$ G248E mutant prepared by in silico replacement of the appropriate amino acid in the crystal structure of $P450_{cam}$, the glutamic acid is positioned close to the 5-methyl of the heme (2.7 Å) (Figure 1 and Table 2). The structure in Figure 1 is the acceptable rotamer with the closest approach of the glutamate to any methyl group on the heme. The carboxyl

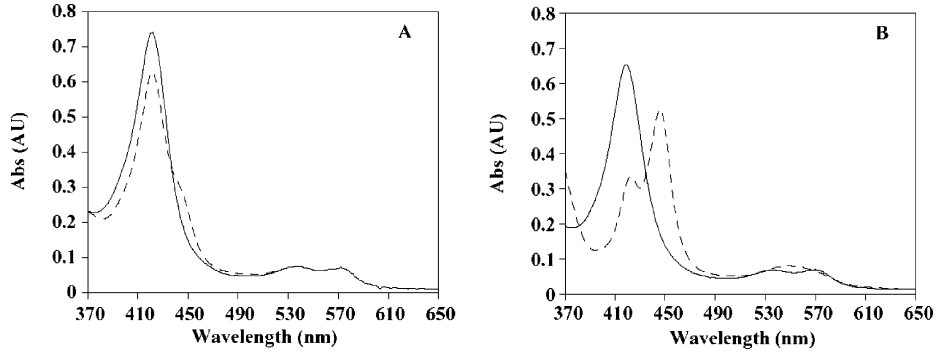

FIGURE 2: Spectroscopic properties of the G248E and G248D P450$_{cam}$ mutants. (A) Ferric G248E P450$_{cam}$ [7 μM in 50 mM potassium phosphate and 100 mM KCl (pH 7.0)] (solid line) and enzyme reduced with dithionite in the presence of CO (dashed line). The latter spectrum is shown after a 2 h anaerobic incubation in the presence of excess dithionite and CO. (B) Ferric G248D P450$_{cam}$ [7 μM in 50 mM potassium phosphate and 100 mM KCl (pH 7.4)] (solid line) and enzyme reduced in the presence of CO (dashed line). The reduced CO spectrum represents a 10 min anaerobic incubation in the presence of excess dithionite and CO.

Table 3: Camphor Binding Constants and Camphor Hydroxylating Activities of Wild-Type, G248E, and G248D P450$_{cam}$

	WT	G248E	G248D
absorbance (nm)			
camphor-free form	417, 532, 568	420, 538, 568	418, 536, 570
camphor-bound form	397, 517, 538, 582	426, 540, 568	426, 546, 572
K_S(camphor) (μM)	1	50 $\pm$ 3	11 $\pm$ 1
activity (no. of turnovers/min)	2154[a]	~0.1	~0.5

[a] From ref *25*.

oxygens sit above the plane of the heme group on the distal side approximately 4.5 Å from the Fe. In the homology-based model of CYP4A11, the glutamic acid oxygen is 7.8 Å from the 5-methyl group of the heme (*24*). When Gly248 is replaced with Asp, the carboxylate oxygen is predicted to be 4.4 Å from the C5 methyl group, as would be expected from the shorter side chain of Asp compared to Glu, and 4.0 Å from the heme iron atom. On the basis of this model, it should be possible for the heme in the G248E and possibly G248A P450$_{cam}$ mutants to bind covalently to the protein if the only requirement for binding is appropriate positioning of the heme.

Protein Expression and Spectroscopic Characterization. The C334A mutant of P450$_{cam}$ was chosen as the starting point for our experiments because removal of this surface cysteine increases the stability of the enzyme (*25*), prevents dimerization (*25*), and allows the protein to run as a single peak on HPLC. Previous studies have shown that the spectral properties and initial rates of camphor hydroxylation by C334A P450$_{cam}$ are identical to those of the wild type (*25*). The C334A P450$_{cam}$ mutant will be called wild type in this paper. In contrast to wild-type P450$_{cam}$, which has a low-spin Fe(III) Soret maximum at 417 nm that shifts to 410 nm upon reduction to the low-spin Fe(II) state, the P450$_{cam}$ G248E mutant exhibited a Soret maximum at 420 nm (Figure 2A and Table 3). Attempts to reduce this enzyme with dithionite did not produce significant changes in the spectrum, suggesting that the protein could not be reduced. The G248D P450$_{cam}$ mutant had a Soret maximum at 418 nm (Figure 2B), and again no significant changes were observed on reduction with dithionite. However, both the G248E and G248D mutants gave rise to reduced CO spectra (λ_{max} = 450 nm) in the presence of dithionite and CO; however, this process was inefficient, and in neither case was a quantitative shift to the 450 nm spectrum obtained (Figure 2B). In the G248E mutant, the Fe(II)−CO complex was observed as a small shoulder that slowly grew in over the course of 2 h. In the G248D mutant, the 450 nm band grew over approximately 10 min with the final spectrum appearing to be a combination of P450 and P420 (Figure 2B). P420 is an inactive form of P450 enzymes in which the axial cysteinate ligand is either protonated or displaced (*29*).

Ligand Binding. The binding constants for camphor were investigated for the P450$_{cam}$ G248E and G248D mutants (Table 3). Camphor binding was perturbed in the mutants as compared to that in wild-type P450$_{cam}$. The Soret band in wild-type P450$_{cam}$ shifted from 417 to 397 nm upon binding of camphor (Figure 3A and Table 3). This shift, along with those of the Q-bands, is characteristic of the conversion of low-spin to high-spin Fe(III). In contrast, both the G248E and G248D mutants of P450$_{cam}$ exhibited small red shifts in their Soret bands upon binding of camphor, and very small changes in the Q-bands (Figure 3B,C and Table 3). The differences between the wild type and G248E and G248D P450$_{cam}$ are further emphasized in the camphor-free minus camphor-bound difference spectra (Figure 3, insets). On the basis of a comparison with the equivalent UV−visible spectra of the A246E mutant of P450$_{BM3}$ (*22*, *23*), the camphor-bound forms of both G248E and G248D P450$_{cam}$ mutants remain predominantly in the six-coordinate low-spin Fe(III) state.

Camphor Hydroxylation Activity. Both G248E and G248D mutants hydroxylate camphor to 5-*exo*-hydroxycamphor, albeit at greatly reduced rates relative to the wild-type enzyme (Table 3). Wild-type P450$_{cam}$ has a turnover number of greater than 2000 min^{-1} (*30*). When expressed as turnover numbers per minute, the activities of both mutants were less that 0.1% of that of the wild type (Table 3). The conversion of camphor to 5-*exo*-hydroxycamphor with the P450$_{cam}$ G248E mutant did not go to completion, with a maximal yield of ~75% after ~3 h (75 μM P450$_{cam}$ G248E and 1.1 mM camphor). The enzyme appeared to be inactive after

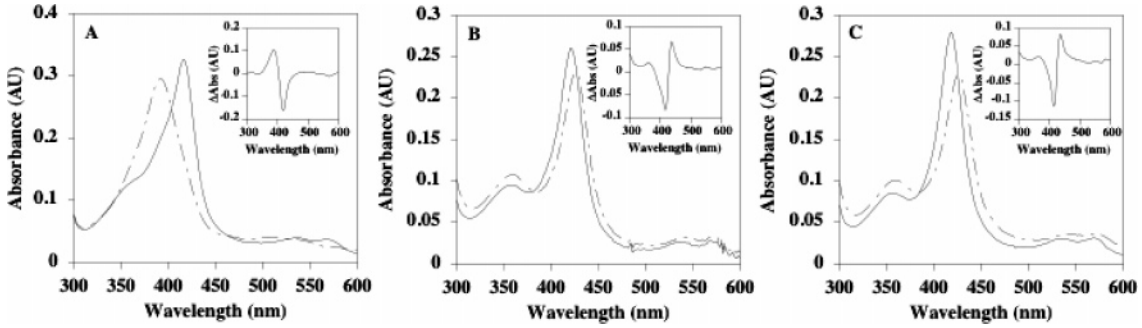

FIGURE 3: Camphor-bound and camphor-free spectra representing camphor binding to (A) wild-type, (B) G248E, and (C) G248D $P450_{cam}$ [5 μM enzyme, 50 mM potassium phosphate, and 100 mM KCl (pH 7.4)]. Insets show the camphor-bound vs camphor-free difference spectra.

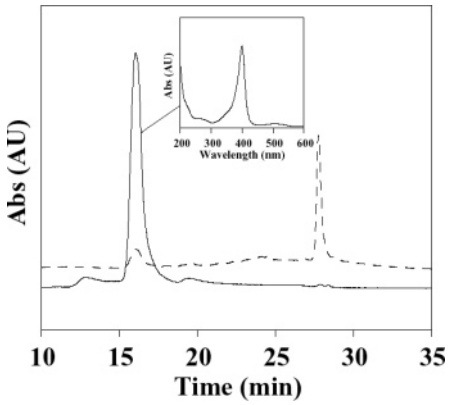

FIGURE 4: HPLC traces of the G248E $P450_{cam}$ mutant (3 nmol) as isolated from the *E. coli* expression system: (solid line) 400 nm trace and (dashed line) 280 nm trace. In the inset is shown the UV−visible spectrum of the 16 min peak with the strong Soret band at 397 nm of free heme.

this time period, and further incubation did not increase the product yield. Thus, despite the low turnover numbers, the mutants retained enough activity to test the effects of the mutations on covalent heme binding.

Autocatalytic Attachment of the Heme. HPLC is a standard way to determine whether a heme prosthetic group is covalently attached to a protein (*14*−*21*). Under denaturing conditions, dissociable heme (monitored at 400 nm) elutes before the polypeptide chain (monitored at 280 nm) on a hydrophobic column, whereas heme that is covalently linked to the protein coelutes with the polypeptide chain. The HPLC of the $P450_{cam}$ G248E mutant, as isolated and purified from the cell paste (Figure 4), showed that the heme elutes as a single peak at 16 min, with only a very small, broad peak representing less than 1% of the heme associated with the polypeptide chain. The spectrum of the free heme has a characteristic Soret band at 397 nm (Figure 4, inset). The corresponding HPLC traces for the G248D mutant were essentially identical to those of wild-type $P450_{cam}$ (data not shown).

When the G248E mutant was incubated with Pd, PdR, catalase, camphor, and NADH, a new peak appears in the 400 nm trace at 28 min (Figure 5A), and this was associated with a protein peak in the 280 nm trace that appeared as a shoulder on the 27 min peak corresponding to heme-free $P450_{cam}$ (Figure 5A). We have attributed this peak to heme covalently bound to $P450_{cam}$, the small change in the hydrophobicity associated with heme attachment giving rise to the slightly delayed elution time. Integration of the two

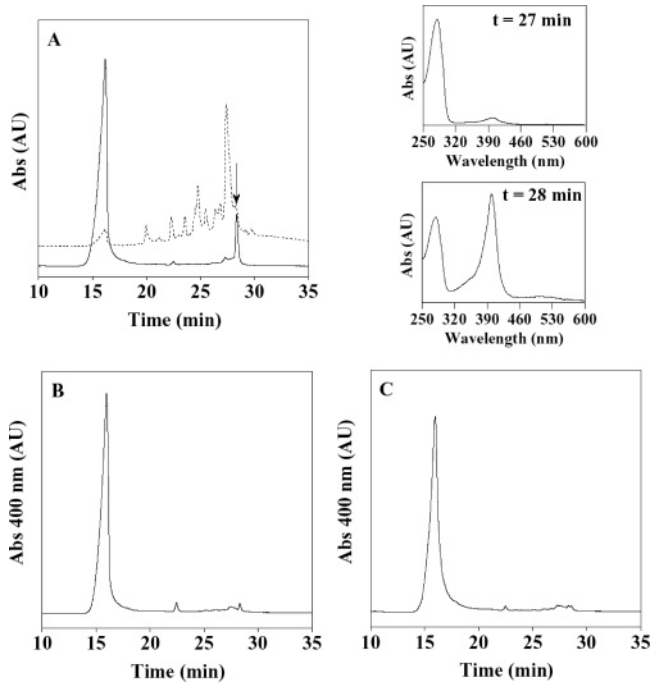

FIGURE 5: HPLC traces of the G248E and G248D $P450_{cam}$ mutants (3 nmol) after catalytic turnover. (A) The 400 (solid line) and 280 nm (dashed line) traces of G248E $P450_{cam}$ after incubation for 3 h at 37 °C in the presence of 30 μM Pd, 15 μM PdR, 2 mM NADH, 1.1 mM camphor, and 1 μM catalase. The spectra to the right show the UV−visible spectra of the peaks at 27 (left) and 28 min (right). The peak assigned as heme bound to $P450_{cam}$ is denoted with the arrow. (B) The 400 nm HPLC trace of G248E $P450_{cam}$ incubated for 3 h at 37 °C under turnover conditions in the absence of camphor (30 μM Pd, 15 μM PdR, 2 mM NADH, and 1 μM catalase). (C) The 400 nm trace of G248D $P450_{cam}$ incubated for 3 h at 37 °C under turnover conditions (30 μM Pd, 15 μM PdR, 2 mM NADH, 1.1 mM camphor, and 1 μM catalase).

heme peaks at 16 and 28 min indicated that 10% of the heme became covalently attached after 3 h when the concentration of $P450_{cam}$ was less than 15 μM. The UV−visible spectra associated with the 27 min (Figure 5A) and 28 min (Figure 5A) peaks confirmed the presence of a significant amount of heme associated with the latter but not the former polypeptide. If camphor was excluded from the reaction, only a trace of the 28 min peak appears (Figure 5B).

When the $P450_{cam}$ G248E mutant was incubated under catalytic conditions, the percentage of covalently bound heme increased with time (Figure 6). This covalent binding was associated with camphor hydroxylation and was nearly complete after 3 h. The linear fit of the time points at 220 min gave a rate for the covalent attachment of 1.1 μM/h (60

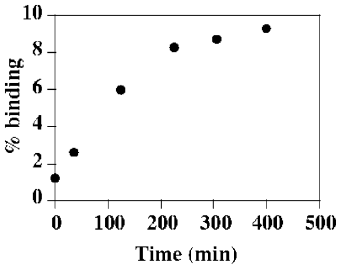

FIGURE 6: Percentage of heme covalently bound to the G248E P450$_{cam}$ protein as a function of time of incubation under turnover conditions at 37 °C (60 μM P450$_{cam}$, 30 μM Pd, 15 μM PdR, 2 mM NADH, 1.1 mM camphor, and 1 μM catalase).

μM G248E P450$_{cam}$). After incubation for 5 h at 37 °C under catalytic conditions, the enzyme was no longer active toward camphor hydroxylation, but after overnight incubation, the percentage of bound heme appeared to increase to as much as 40% of the final heme content (data not shown). This apparent increase in the amount of bound heme was accompanied by a significant bleaching of the total recovered heme (bound plus unbound), complicating interpretation of the slow increase in the fraction of bound heme observed at long time periods. Bleaching can be assessed by calculating the total areas of the peaks in the 400 nm HPLC traces prior to and after covalent attachment. We have not investigated the source of this bleaching, a reaction that is well-known in the hemoprotein field (e.g., ref *31*), but have restricted the time frame of our studies to <5 h, during which the amount of bleaching was not significant (<5%) and the enzyme retained catalytic activity.

In the CYP4 enzymes, mutation of the glutamate that covalently links the heme to an aspartate alters the outcome of the covalent attachment process (*17*). As an aspartate is shorter than a glutamate, the formation of the covalent link becomes less efficient but oxidation of the C5 methyl group of the heme continues unabated (*17*), resulting in the formation of noncovalently bound 5-HO heme in which the carbocation intermediate (Scheme 2) is trapped by water rather than by the carboxylate group. This species is more polar than native heme and elutes earlier than heme on reverse-phase HPLC (*17*). Since the P450$_{cam}$ G248E mutant was able to covalently bind heme, the G248D mutant was also subjected to HPLC analysis after incubation under turnover conditions. In contrast to the G248E mutant, no heme eluted with the G248D protein peak (Figure 5C), and no new peaks indicative of the formation of hydroxylated hemes were observed in the 400 nm HPLC trace.

Digestion of the P450$_{cam}$ G248E Mutant. Pronase digestion of heme proteins in which the heme is attached to the peptide via an ester linkage to a heme methyl can be used to identify the position of covalent attachment (*14*). Figure 7B shows the result of digesting recombinant wild-type CYP4A3 in which 30% of the heme was attached to the protein as purified from the expression system (*14*). There are two peaks in the HPLC trace at 27 and 32 min. Previous studies have shown that the four possible hydroxymethyl derivatives of heme are separated by the HPLC system employed here (*21*). The peak at 27 min represents 5-HO heme and the peak at 32 min free heme. A digest of the G248E mutant in which 10% of the heme was attached to the protein yielded a trace similar to that observed for CYP4A3, consistent with the formation of 5-OH heme (Figure 7A). The peak at 27 min is clearly lower for G248E P450$_{cam}$ than for CYP4A3, consistent with the lower extent of covalently bound heme in the starting P450$_{cam}$ G248E sample.

To positively identify the 27 min peak in Figure 7, the digested samples of CYP4A3 and P450$_{cam}$ G248E were analyzed by LC−MS. The insets in Figure 7 clearly show that the mass of the 27 min peak is that of a monohydroxylated heme (632 amu instead of 616 amu). Both the elution time and the mass of the product seen following digestion of heme-bound G248E are consistent with the formation of 5-HO heme. These findings imply that the heme is bound in the G248E P450$_{cam}$ mutant via an ester linkage between the carboxylate side chain of Glu248 and the 5-methyl of the heme.

DISCUSSION

The UV−visible spectra of the P450$_{cam}$ G248E and G248D mutants, like that of the wild-type enzyme, indicate that the resting forms of the enzymes are low-spin Fe(III) (Figure 2). However, once camphor binds, the spectra of the mutants differ significantly from that of the wild type (Figure 3). The high-spin five-coordinate Fe(III) state of camphor-bound wild-type P450$_{cam}$ is characterized by a Soret band at 397 nm and a broad Q-band centered at 550 nm. In contrast, the Soret bands of the G248E and G248D mutants upon binding of camphor are red shifted and the α and β bands remain well resolved. As judged from the spectroscopic substrate binding assay (Table 3), camphor binds more weakly to the mutant proteins than to the wild type. This suggests that the carboxylate side chain forces the heme to remain in the low-spin Fe(III) state even when camphor is bound. Recent work

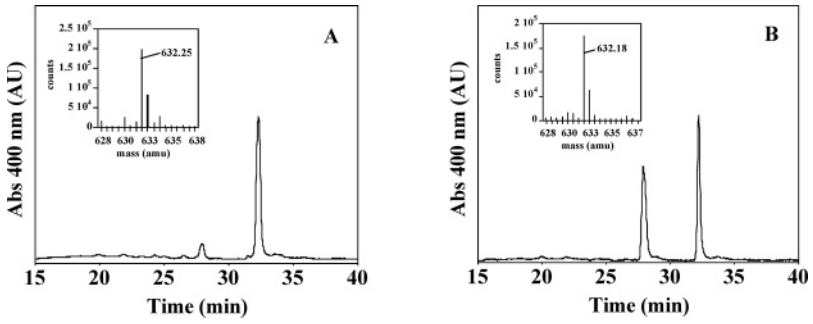

FIGURE 7: Comparison of the covalently bound hemes from G248E P450$_{cam}$ after incubation under turnover conditions and wild-type CYP4A1. (A) The 400 nm trace of Pronase-digested G248E P450$_{cam}$ (3 nmol) in which 10% of the heme was covalently attached. (B) The 400 nm trace of Pronase-digested recombinant CYP4A1 (1 nmol) as isolated. In the insets are the mass spectra of the peaks at 12 min (5 HO-heme) in the LC−MS traces of Pronase-digested G248E P450$_{cam}$ (inset in A) or wild-type CYP4A1 (inset in B), where these peaks correspond to the 28 min peaks in panels A and B (see Experimental Procedures).

on the A246E mutant of $P450_{BM3}$ showed that in the resting state the iron is largely coordinated to the glutamate carboxyl group and the overall conformation of the enzyme is close to that of the substrate-bound form even though the iron remains low-spin (*22*, *23*). Once a fatty acid substrate has bound, the glutamate carboxylate is bound to the heme to an even greater extent. Despite this ligation, the A246E $P450_{BM3}$ mutant retains significant activity but does not give rise to heme covalent binding. The UV−visible spectral characteristics of the $P450_{cam}$ G248E and G248D mutants are very similar to those of the A246E $P450_{BM3}$ mutant, as expected if the carboxylate also coordinates to the heme iron atom in the $P450_{cam}$ mutants.

Compared to that of the wild-type enzyme, binding of CO to both P450 mutants under reducing conditions is very slow, and in the case of the G248E $P450_{cam}$ mutant, no more than a fraction of the protein can be converted to the CO-bound state. Access to the distal pocket in the G248E mutant appears to be much more limited than in the wild-type enzyme, with the G248D mutant lying somewhere between the two. This is reflected in the 50-fold weaker binding of camphor to the G248E than to the wild-type protein and the greatly reduced activity of the former (Table 3). The changes in properties caused by the mutation reflect, at least in part, coordination of the glutamate to the iron even in the substrate-bound state, in analogy to the results found with $P450_{BM3}$ (*22*, *23*). An aspartate at position 248 behaves in a similar fashion, but with somewhat smaller effects on substrate affinity and catalytic activity. The modeling studies readily explain why the Glu248 binds heme covalently but the Asp248 does not, but they do not explain why the Asp248 mutation has weaker effects on substrate binding and catalysis (Table 3). Thus, the Glu248 carboxyl can approach the 5-methyl more closely than the carboxyl of Asp248 (Table 2), but both carboxyls place an oxygen approximately the same distance (4.0−4.5 Å) from the Fe. However, the structure modeling is based on the side chain rotomer with the closest approach of the carboxylate to the 5-methyl, and alternative rotamer positions are possible.

The observation of camphor hydroxylation with both the G248E and G248D $P450_{cam}$ mutants shows that both enzymes are capable, albeit slowly, of producing the activated ferryl radical cation species. This is an essential step in the proposed autocatalytic mechanism for covalent attachment of the heme in the CPY4 enzymes (*17*, *18*). HPLC analysis of the G248D $P450_{cam}$ mutant after turnover showed the presence of only free unmodified heme, but similar analysis of the G248E mutant showed that up to 10% of the heme became attached to the protein during camphor hydroxylation. The heme is attached via its 5-methyl substituent, as found in the CYP4A enzymes (*17*) and as predicted by the model used to design the mutant (Figure 1 and Table 1). Complete pronase digestion of the G248E $P450_{cam}$ mutant following turnover releases 5-HO heme (Figure 7), again as found for CYP4A8 (*17*). The $P450_{cam}$ G248E mutant is thus a mimic of the CYP4A enzymes, and the observation of covalent binding of the heme upon introduction of a carboxyl into a protein with a very low level of sequence identity indicates that the ability to covalently bind the heme group *is unlikely to require additional specific active site assistance*. The lower extent of heme covalent binding in the $P450_{cam}$ G248E mutant (10%) than in the CYP4 enzymes (>95%) clearly reflects the low catalytic activity of the mutant enzyme, which is largely determined by a nonoptimal positioning of the carboxyl group that allows its coordination to the heme iron. Recombinant CYP4A enzymes that have less than 50% of the heme covalently attached have been isolated, but the spectra of these enzymes indicate that the carboxylate side chain in these proteins is not coordinated to the iron atom (*14*−*17*). After catalytic turnover of the recombinant CYP4 proteins, something approaching quantitative heme covalent binding is achieved. It is not surprising that the CYP4A active sites have been fine-tuned to position the carboxylate at precisely the right distance to prevent iron coordination and yet allow trapping of the cationic heme intermediate, whereas this has not been achieved in the $P450_{cam}$ mutants. This is also illustrated by the failure of the corresponding $P450_{BM3}$ mutant to covalently bind the heme at all (*22*, *23*). It should be noted, however, that coordination of the glutamate carboxylate to the heme iron may be prevented in the CYP4 enzymes not only by positioning but also by secondary mechanisms such as hydrogen bonding interactions.

The failure to detect either covalent binding or modification of the heme methyl in the G248D mutant indicates that the aspartate carboxyl group is incorrectly placed for reaction with the heme methyl. In the case of the CYP4 enzymes, mutation of the normal glutamate to an aspartate results in methyl oxidation but not covalent binding because water now competes effectively with the carboxylate for trapping of the carbocation (*17*). Thus, a small shift in the position of the carboxyl in enzymes evolved to carry out the reaction results in dissociation of methyl oxidation from heme covalent binding. In this situation, the aspartate mutant is 5-fold more active in the oxidation of camphor, presumably because it coordinates less tightly to the heme iron. However, the aspartate in the mutant is unable to abstract the hydrogen from the heme methyl group. The model of the G248D mutant (Table 3) suggests that the aspartate carboxyl oxygens are positioned ∼2 Å further from the heme C5 methyl group than the corresponding glutamate carboxyl oxygen in the G248E mutant. The aspartate in the G248D mutant is thus positioned so that it is either not oxidized to the radical or not able to abstract a hydrogen from the heme methyl. Incorrect positioning is clearly related to the difference in the lengths of the aspartate and glutamate side chains, as well as to the fact that the side chains are flexible and could differentially interact with other active site residues. In the absence of actual crystal structures, it is not possible to precisely define why one chain length works and the other does not.

Covalent attachment of the heme in the G248E $P450_{cam}$ mutant provides strong support for the proposed mechanism for formation of a heme−protein ester bond in the CYP4 enzymes. The activated ferryl intermediate appears to have an inherent ability to activate an appropriately placed carboxylate side chain. No unusual properties of the active site are required for formation of the ester bond, although interactions of the carboxyl group could help prevent its coordination to the heme iron atom. This result concurs with our observations on the mammalian peroxidases (*19*−*21*), and with our finding that introduction of a carboxyl side chain into horseradish peroxidase results, as in the mammalian peroxidases, in the formation of a heme−protein

covalent link (*21*). We have also recently demonstrated that horseradish peroxidase can oxidize acetic acid to a carboxyl free radical species that adds to the meso carbon of the heme but also, to a small extent, converts the heme to a hydroxymethylheme (*32*). Thus, although the active site species in the peroxidases and P450 enzymes are considerably different, the collective evidence indicates that in the P450 enzymes, as in the peroxidases, the formation of a covalent bond between a heme methyl and a protein carboxyl group is primarily the result of propinquity and requires no active assistance by protein residues other than the carboxyl group involved in the reaction.

REFERENCES

1. Guengerich, F. P. (2004) Human cytochrome P450 enzymes, in *Cytochrome P450: Structure, Mechanism, and Biochemistry*, 3rd ed. (Ortiz de Montellano, P. R., Ed.) pp 377−530, Plenum-Klewer, New York.
2. Kelly, S. L., Kelly, D. E., Jackson, C. J., Warrilow, A. G. S., and Lamb, D. C. (2004) The diversity and importance of microbial cytochromes P450, in *Cytochrome P450: Structure, Mechanism, and Biochemistry*, 3rd ed. (Ortiz de Montellano, P. R., Ed.) pp 585−617, Plenum-Klewer, New York.
3. Nielsen, K. A., and Møller, B. L. (2004) Cytochrome P450s in plants, in *Cytochrome P450: Structure, Mechanism, and Biochemistry*, 3rd ed. (Ortiz de Montellano, P. R., Ed.) pp 553−583, Plenum-Klewer, New York.
4. Poulos, T. L., Finzel, B. C., and Howard, A. J. (1987) High-resolution crystal structure of cytochrome $P450_{cam}$, *J. Mol. Biol. 195*, 687−700.
5. Schlichting, I., Berendzen, J., Chu, K., Stock, A. M., Maves, S. A., Benson, D. E., Sweet, R. M., Ringe, D., Petsko, G. A., and Sligar, S. G. (2000) The catalytic pathway of cytochrome $P450_{cam}$ at atomic resolution, *Science 287*, 1615−1622.
6. Makris, T. M., Denisov, I., Schlichting, I., and Sligar, S. G. (2004) Activation of molecular oxygen by cytochrome P450, in *Cytochrome P450: Structure, Mechanism, and Biochemistry*, 3rd ed. (Ortiz de Montellano, P. R., Ed.) pp 149−182, Plenum-Klewer, New York.
7. Paine, M. J. I., Scrutton, N. S., Munro, A. W., Gutierrez, A., Roberts, G. C. K., and Wolf, C. R. (2004) Electron transfer partners of cytochrome P450, in *Cytochrome P450: Structure, Mechanism, and Biochemistry*, 3rd ed. (Ortiz de Montellano, P. R., Ed.) pp 115−148, Plenum-Klewer, New York.
8. Roome, P. W., Jr., Philley, J. C., and Peterson, J. A. (1983) Purification and properties of putidaredoxin reductase, *J. Biol. Chem. 258*, 2593−2598.
9. Tanaka, M., Hanu, M., Yasunobu, K. T., Dus, K., and Gunsalus, I. C. (1974) Amino acid sequence of putidaredoxin, an iron−sulfur protein from *Pseudomonas putida*, *J. Biol. Chem. 249*, 3689−3701.
10. Davydov, D., Hoa, G., and Peterson, J. (1999) Dynamics of protein-bound water in the heme domain of $P450_{BM3}$ studied by high-pressure spectroscopy: Comparison with $P450_{cam}$ and P450 2B4, *Biochemistry 38*, 751−761.
11. Tosha, T., Yoshioka, S., Takahashi, S., Ishimori, K., Shimada, H., and Morishima, I. (2003) NMR study on the structural changes of cytochrome $P450_{cam}$ upon the complex formation with putidaredoxin. Functional significance of the putidaredoxin-induced structural changes, *J. Biol. Chem. 278*, 39809−39821.
12. Sligar, S. G., and Gunsalus, I. C. (1976) A thermodynamic model of regulation: Modulation of redox in camphor monoxygenase, *Proc. Natl. Acad. Sci. U.S.A. 73*, 1078−1082.
13. Ortiz de Montellano, P. R., and De Voss, J. (2004) Substrate oxidation by cytochrome P450 enzymes, in *Cytochrome P450: Structure, Mechanism, and Biochemistry*, 3rd ed. (Ortiz de Montellano, P. R., Ed.) pp 183−245, Plenum-Klewer, New York.
14. Hoch, U., and Ortiz de Montellano, P. R. (2001) Covalently-linked heme in cytochrome P4504A fatty acid hydroxylases, *J. Biol. Chem. 276*, 11339−11346.
15. Henne, K. R., Kunze, K. L., Zheng, Y. M., Christmas, P., Soberman, R. J., and Rettie, A. E. (2001) Covalent linkage of prosthetic heme to CYP4 family P450 enzymes, *Biochemistry 40*, 12925−12931.
16. LeBrun, L. A., Xu, F., Kroetz, D. L., and Ortiz de Montellano, P. R. (2002) Covalent attachment of the heme prosthetic group in the CYP4F cytochrome P450 family, *Biochemistry 41*, 5931−5937.
17. Lebrun, L. A., Hoch, U., and Ortiz de Montellano, P. R. (2002) Autocatalytic mechanism and consequences of covalent heme attachment in the cytochrome P4504A family, *J. Biol. Chem. 277*, 12755−12761.
18. Zheng, Y.-M., Baer, B. R., Kneller, M. B., Henne, K. R., Kunze, K. L., and Rettie, A. E. (2003) Covalent heme binding to CYP4B1 via Glu310 and a carbocation porphyrin intermediate, *Biochemistry 42*, 4601−4606.
19. DePillis, G. D., Ozaki, S., Kuo, J. M., Maltby, D. A., and Ortiz de Montellano, P. R. (1997) Autocatalytic processing of heme by lactoperoxidase produces the native protein-bound prosthetic group, *J. Biol. Chem. 272*, 8857−8860.
20. Colas, C., Kuo, J. M., and Ortiz de Montellano, P. R. (2002) Asp225 and Glu375 in autocatalytic attachment of the prosthetic heme group of lactoperoxidase, *J. Biol. Chem. 277*, 7191−7200.
21. Colas, C., and Ortiz de Montellano, P. R. (2004) Horseradish peroxidase mutants that autocatalytically modify their prosthetic heme group. Insights into mammalian peroxidase heme-protein covalent bonds, *J. Biol. Chem. 279*, 24131−24140.
22. Joyce, M. G., Girvan, H. M., Munro, A. W., and Leys, D. (2004) A single mutation in cytochrome $P450_{BM3}$ induces the conformational rearrangement seen upon substrate binding in the wild-type enzyme, *J. Biol. Chem. 279*, 23287−23293.
23. Girvan, H. M., Marshall, K. R., Lawson, R. J., Leys, D., Joyce, M. G., Clarkson, J., Smith, W. E., Cheesman, M. R., and Munro, A. W. (2004) Flavocytochrome $P450_{BM3}$ mutant A264E undergoes substrate-dependent formation of a novel heme iron ligand set, *J. Biol. Chem. 279*, 23274−23286.
24. Chang, Y., and Loew, G. (1999) Homology modeling and substrate binding study of human CYP4A11 enzyme, *Proteins: Struct., Funct., Genet. 34*, 403−415.
25. Nickerson, D., and Wong, L. (1997) The dimerization of *Pseudomonas putida* cytochrome $P450_{cam}$: Practical consequences and engineering of a monomeric enzyme, *Protein Eng. 10*, 1357−1361.
26. De Voss, J. J., Sibbesen, O., Zhang, Z., and Ortiz de Montellano, P. R. (1997) Substrate docking algorithms and prediction of the substrate specificity of cytochrome $P450_{cam}$ and its L244A mutant, *J. Am. Chem. Soc. 119*, 5489−5498.
27. Omura, T., and Sato, R. (1964) The carbon monoxide-binding pigment of liver microsomes. I. Evidence for its hemoprotein nature, *J. Biol. Chem. 239*, 2370−2378.
28. Kadkhodayan, S., Coulter, E. D., Maryniak, D. M., Bryson, T. A., and Dawson, J. H. (1995) Uncoupling oxygen transfer and electron transfer in the oxygenation of camphor analogues by cytochrome $P450_{cam}$, *J. Biol. Chem. 270*, 28042−28048.
29. Perera, R., Sono, M., Sigman, J. A., Pfister, T. D., Lu, Y., and Dawson, J. H. (2003) Neutral thiol as a proximal ligand to ferrous heme iron: Implications for heme proteins that lose cysteine thiolate ligation on reduction, *Proc. Natl. Acad. Sci. U.S.A. 100*, 3641−3646.
30. Ullah, A. J. H., Murray, R. I., Bhattacharyya, P. K., Wagner, G. C., and Gunsalus, I. C. (1990) Protein components of a cytochrome P450 linalool 8-methyl hydroxylase, *J. Biol. Chem. 265*, 1345−1351.
31. Schefer, W. H., Harris, T. M., and Guengerich, F. P. (1985) Characterization of the enzymatic and non-enzymatic peroxidative degradation of iron porphyrins and cytochrome P450 heme, *Biochemistry 24*, 3254−3263.
32. Huang, L., Colas, C., and Ortiz de Montellano, P. R. (2004) Oxidation of carboxylic acids by horseradish peroxidase results in prosthetic heme modification and inactivation, *J. Am. Chem. Soc. 126*, 12865−12873.
33. Delano, W. L. (2002) *The Pymol Molecular Graphics System*, DeLano Scientific, South San Francisco, CA.

BI047686I